
EASR

Engineering and Applied Science Research<https://www.tci-thaijo.org/index.php/easr/index>Published by the Faculty of Engineering, Khon Kaen University, Thailand

Development of frame finite element model for truss structures with semi-rigid connectionsNatee Panagant^{*1)}, Sujin Bureerat¹⁾ and Kang Tai²⁾¹⁾Sustainable and Infrastructure Research and Development Center, Department of Mechanical Engineering, Faculty of Engineering, Khon Kaen University, Khon Kaen 40002, Thailand²⁾School of Mechanical and Aerospace Engineering, Nanyang Technological University, 50 Nanyang Ave, 639798, Singapore

Received 21 Feb 2018

Accepted 30 Mar 2018

Abstract

The problem of connecting truss structures is one of the major concerns in structural analysis and design. The behavior of truss structures is usually analyzed using a common finite element model, which considers each member as a two-force member. Each truss member connection is treated as a rotational pinned joint, but in the reality, the members of truss structures are usually connected with bolts or by welding. Alternatively, a designer may analyze such a structure using a frame finite element model where joint connections are considered fixed or rigid connections, which provide a connection that is stiffer than the inherent behavior. In this research, instead of using truss or frame finite element models, a substructure technique is employed to develop a more realistic finite element model. Each element is separated into three parts, a main element and two joint elements. The substructure technique is integrated into the frame finite element model to reduce design variables in global equations, to increase deformability of the joint elements, and make the proposed model more realistic. Young's modulus values of the joints are reduced as a percentage of the modulus of the main elements. Comparison of the results obtained from the proposed model to the truss and frame finite element models are reported.

Keywords: Finite element method, Semi-rigid, Partially restrained, Flexible connections, Substructure

1. Introduction

The finite element method is one of the most popular numerical methods for solving engineering problems, especially solid mechanics problems. Many recent works employed finite element methods to solve engineering problems [1-2]. Truss structures are one of the most widely used types of structures. There has been much research related to truss structures [3-6]. While each member of a truss structure is commonly considered a two-force member that supports only an axial load, real truss structures are usually assembled by bolts or welded connections that also supported bending moments and shear loadings. In general finite element analyses [7-8], a truss element is considered a two-force member while a frame element also carries moments and shear loadings. Connections of both truss and frame finite element models are usually assumed as rotationally pinned and fixed connections, respectively. Real truss structures with bolts or welded connections are not rigid. In fact, their connections are deformable. Thus, the behavior of the real truss structures should be more similar to the frame finite element model with non-rigid connections. Semi-rigid connections, which are also called partially-restrained/flexible connections, have received much interest over the past few decades. There have been many studies attempting to examine such behavior and

developing numerical models of semi-rigid connections. In 1986, Lui and Chen [9] developed one of the earliest finite element methods for frame structures with semi-rigid connections. Then, Suarez, Singh, and Matheu [10] developed a new finite element method to examine seismic responses of frame structures with semi-rigid connections in 1996. In 2003, Hadianfard and Razani [11] performed reliability analysis of frame structures with semi-rigid connections using the finite element method. Thereafter, there were a great number of studies on the behavior of frame structures with semi-rigid connections [12-20]. There has been some interesting work in multi-component structural design and optimization [21-22]. These structures are considered as several components, with the frame components connected by spot welded joints and considered as torsion spring connections in finite element analysis.

Although there has been much research on semi-rigid connections, most studies focused on steel frame structures and vibration analysis [13-20]. In this article, a substructure technique was integrated into a frame finite element model to develop a semi-rigid frame finite element to perform stress and displacement analysis of both planar and space truss structures. The substructure technique is known by a few different names, including super-element and static/dynamic condensation. A few decades ago, computing capability and memory of microcomputers were very limited compared to

*Corresponding author. Tel.: +6692 291 5326

Email address: natee_panagant@kkumail.com

doi: 10.14456/easr.2018.25

recent times. The substructure technique was employed to make it possible to solve large-scale problems with limited memory [23]. After separating the domain into two or more parts, algebraic or global equations of a finite element method need to be re-formulated as demonstrated in [24-25]. Although modern personal computers are a lot faster compared to those from a few decades ago, solving large-scale problems or optimization problems that require a great number of evaluations can still require a lot of computational time. In this article, the authors increase the detail of the domain by subdividing each truss element into one main element and two joint elements. The number of elements of the new model was increased by three times over that of a general frame finite element model. Most of the computational effort in finite element analysis is in matrix inversion. Therefore, a substructure technique is employed to group a main element and both joints together to maintain the same number of degrees of freedom in the global finite element equations.

The details of finite element formulation of the welding truss model are demonstrated in the next section. Results, discussion and conclusions are included in Sections 3, 4, and 5, respectively.

2. Materials and methods

2.1 Frame finite element model

In this article, a new semi-rigid connection frame finite element model is developed. Each general frame element is subdivided into three parts, one main element and two joint elements. Instead of performing common finite element

analysis with additional elements, the main element and both joint elements are grouped together. Then, the substructure technique [24-25] is employed to derive a new element stiffness matrix and maintain the same number of degrees of freedom in a global finite element stiffness matrix.

The frame finite element method employed is from [8]. There are 12 degrees of freedom for the frame element as shown in Figure 1. Here, *x*, *y*, and *z*-axes are local Cartesian coordinates, *q*₁, *q*₂, and *q*₃ are translation displacements of node (I), *q*₇, *q*₈, and *q*₉ are translation displacements of node (J), *q*₄, *q*₅, and *q*₆ are rotational displacements of node (I) and *q*₁₀, *q*₁₁, and *q*₁₂ are rotational displacements of node (J). Each translation or rotational displacement is a response to their applied loads (*F*₁-*F*₁₂). The translation displacements respond to forces while rotational displacements respond to moments.

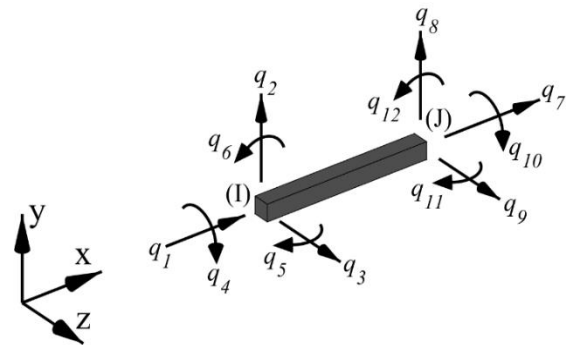


Figure 1 Detail of degrees of freedom of a frame element

The frame finite element equations of each element are provided by equation (1).

$$K_{12 \times 12}^e \delta_{12 \times 1}^e = F_{12 \times 1}^e \tag{1}$$

where $K_{12 \times 12}^e$ is a stiffness matrix of the element *e*, $\delta_{12 \times 1}^e$ is a nodal displacement vector of the element *e*, and $F_{12 \times 1}^e$ is a nodal load vector of the element *e*. More details of $K_{12 \times 12}^e$, $\delta_{12 \times 1}^e$, and $F_{12 \times 1}^e$ are described by equation (2).

$$\begin{bmatrix} \frac{AE}{L} & 0 & 0 & 0 & 0 & 0 & -\frac{AE}{L} & 0 & 0 & 0 & 0 & 0 \\ 0 & \frac{12EI_z}{L^3} & 0 & 0 & 0 & \frac{6EI_z}{L^2} & 0 & -\frac{12EI_z}{L^3} & 0 & 0 & 0 & \frac{6EI_z}{L^2} \\ 0 & 0 & \frac{12EI_y}{L^3} & 0 & 0 & \frac{6EI_y}{L^2} & 0 & 0 & -\frac{12EI_y}{L^3} & 0 & \frac{6EI_y}{L^2} & 0 \\ 0 & 0 & 0 & \frac{GJ}{L} & 0 & 0 & 0 & 0 & 0 & -\frac{GJ}{L} & 0 & 0 \\ 0 & 0 & \frac{6EI_y}{L^2} & 0 & \frac{4EI_y}{L} & 0 & 0 & 0 & -\frac{6EI_y}{L^2} & 0 & \frac{2EI_y}{L} & 0 \\ 0 & \frac{6EI_z}{L^2} & 0 & 0 & 0 & \frac{4EI_z}{L} & 0 & -\frac{6EI_z}{L^2} & 0 & 0 & 0 & \frac{2EI_z}{L} \\ -\frac{AE}{L} & 0 & 0 & 0 & 0 & 0 & \frac{AE}{L} & 0 & 0 & 0 & 0 & 0 \\ 0 & -\frac{12EI_z}{L^3} & 0 & 0 & 0 & -\frac{6EI_z}{L^2} & 0 & \frac{12EI_z}{L^3} & 0 & 0 & 0 & -\frac{6EI_z}{L^2} \\ 0 & 0 & -\frac{12EI_y}{L^3} & 0 & -\frac{6EI_y}{L^2} & 0 & 0 & 0 & \frac{12EI_y}{L^3} & 0 & -\frac{6EI_y}{L^2} & 0 \\ 0 & 0 & 0 & -\frac{GJ}{L} & 0 & 0 & 0 & 0 & 0 & \frac{GJ}{L} & 0 & 0 \\ 0 & 0 & \frac{6EI_y}{L^2} & 0 & \frac{2EI_y}{L} & 0 & 0 & 0 & -\frac{6EI_y}{L^2} & 0 & \frac{4EI_y}{L} & 0 \\ 0 & \frac{6EI_z}{L^2} & 0 & 0 & 0 & \frac{2EI_z}{L} & 0 & -\frac{6EI_z}{L^2} & 0 & 0 & 0 & \frac{4EI_z}{L} \end{bmatrix} \begin{Bmatrix} q_1 \\ q_2 \\ q_3 \\ q_4 \\ q_5 \\ q_6 \\ q_7 \\ q_8 \\ q_9 \\ q_{10} \\ q_{11} \\ q_{12} \end{Bmatrix} = \begin{Bmatrix} F_1 \\ F_2 \\ F_3 \\ F_4 \\ F_5 \\ F_6 \\ F_7 \\ F_8 \\ F_9 \\ F_{10} \\ F_{11} \\ F_{12} \end{Bmatrix} \tag{2}$$

where *A* is the cross-section area of the element, *L* is length of the element, *E* is Young’s modulus, *I_y* and *I_z* are area moments of inertia of the cross-section about local *y* and *z* coordinates respectively, *G* is shear modulus, and *J* is torsional constant. For convenience of further demonstration, the stiffness matrix ($K_{12 \times 12}^e$) is split into four parts while displacements ($\delta_{12 \times 1}^e$) and loads ($F_{12 \times 1}^e$) of node (I) and node (J) are separated as described in equation 3.

$$\begin{bmatrix} K_{11}^e & K_{12}^e \\ K_{21}^e & K_{22}^e \end{bmatrix} \begin{Bmatrix} \delta_{(I)}^e \\ \delta_{(J)}^e \end{Bmatrix} = \begin{Bmatrix} F_{(I)}^e \\ F_{(J)}^e \end{Bmatrix} \tag{3}$$



Figure 2 Common frame element (left) and frame finite element with 2 split joints (right)

2.2 Substructure technique

In this article, the common finite element is subdivided into three parts, as demonstrated in Figure 2, to achieve a more realistic model. The number of elements in the new semi-rigid frame model is three times that of the common frame finite element model. As a result, a substructure technique is employed to reduce computational effort in the stiffness matrix inversion process. With this technique, three sub-elements are merged to create 1 combined element, so that the degrees of freedom in the global finite element equations of the semi-rigid frame model remain equal to that of the common frame model.

The frame finite element equations of elements $j1$, e , and $j2$ are described in equations (4), (5), and (6), respectively. External loads are only applied to external nodes (I) and (J), so that load vectors corresponding to nodes (K) and (L) in equation (4-6) are equal to zero.

$$\begin{bmatrix} K_{11}^{(j1)} & K_{12}^{(j1)} \\ K_{21}^{(j1)} & K_{22}^{(j1)} \end{bmatrix}_{6 \times 6} \begin{Bmatrix} \delta_{(I)6 \times 1} \\ \delta_{(K)6 \times 1} \end{Bmatrix} = \begin{Bmatrix} F_{(I)6 \times 1} \\ \mathbf{0} \end{Bmatrix} \quad (4)$$

$$\begin{bmatrix} K_{11}^{(e)} & K_{12}^{(e)} \\ K_{21}^{(e)} & K_{22}^{(e)} \end{bmatrix}_{6 \times 6} \begin{Bmatrix} \delta_{(K)6 \times 1} \\ \delta_{(L)6 \times 1} \end{Bmatrix} = \begin{Bmatrix} \mathbf{0} \\ \mathbf{0} \end{Bmatrix} \quad (5)$$

$$\begin{bmatrix} K_{11}^{(j2)} & K_{12}^{(j2)} \\ K_{21}^{(j2)} & K_{22}^{(j2)} \end{bmatrix}_{6 \times 6} \begin{Bmatrix} \delta_{(L)6 \times 1} \\ \delta_{(J)6 \times 1} \end{Bmatrix} = \begin{Bmatrix} \mathbf{0} \\ F_{(J)6 \times 1} \end{Bmatrix} \quad (6)$$

Then equations (4-6) are assembled to form a system of equations of combined elements as shown in equation (7).

$$\begin{bmatrix} K_{11}^{(j1)} & K_{12}^{(j1)} & 0 & 0 \\ K_{21}^{(j1)} & K_{22}^{(j1)} + K_{11}^{(e)} & K_{12}^{(e)} & 0 \\ 0 & K_{21}^{(e)} & K_{22}^{(e)} + K_{11}^{(j2)} & K_{12}^{(j2)} \\ 0 & 0 & K_{21}^{(j2)} & K_{22}^{(j2)} \end{bmatrix}_{24 \times 24} \begin{Bmatrix} \delta_{(I)6 \times 1} \\ \delta_{(K)6 \times 1} \\ \delta_{(L)6 \times 1} \\ \delta_{(J)6 \times 1} \end{Bmatrix} = \begin{Bmatrix} F_{(I)6 \times 1} \\ \mathbf{0} \\ \mathbf{0} \\ F_{(J)6 \times 1} \end{Bmatrix} \quad (7)$$

Then, lines 1-2 and lines 3-4 of the system of equations (7) are split into equations (8) and (9) respectively.

$$\begin{bmatrix} K_{21}^{(j1)} & \mathbf{0} \\ \mathbf{0} & K_{12}^{(j2)} \end{bmatrix}_{12 \times 12} \begin{Bmatrix} \delta_{(I)6 \times 1} \\ \delta_{(J)6 \times 1} \end{Bmatrix} + \begin{bmatrix} K_{22}^{(j1)} + K_{11}^{(e)} & K_{12}^{(e)} \\ K_{21}^{(e)} & K_{22}^{(e)} + K_{11}^{(j2)} \end{bmatrix}_{12 \times 12} \begin{Bmatrix} \delta_{(K)6 \times 1} \\ \delta_{(L)6 \times 1} \end{Bmatrix} = \begin{Bmatrix} \mathbf{0} \\ \mathbf{0} \end{Bmatrix} \quad (8)$$

$$\begin{bmatrix} K_{11}^{(j1)} & \mathbf{0} \\ \mathbf{0} & K_{22}^{(j2)} \end{bmatrix}_{12 \times 12} \begin{Bmatrix} \delta_{(I)6 \times 1} \\ \delta_{(J)6 \times 1} \end{Bmatrix} + \begin{bmatrix} K_{12}^{(j1)} & \mathbf{0} \\ \mathbf{0} & K_{21}^{(j2)} \end{bmatrix}_{12 \times 12} \begin{Bmatrix} \delta_{(K)6 \times 1} \\ \delta_{(L)6 \times 1} \end{Bmatrix} = \begin{Bmatrix} F_{(I)6 \times 1} \\ F_{(J)6 \times 1} \end{Bmatrix} \quad (9)$$

Equation (8) is re-derive to use the relation, $\begin{Bmatrix} \delta_{(K)6 \times 1} \\ \delta_{(L)6 \times 1} \end{Bmatrix}$ and $\begin{Bmatrix} \delta_{(I)6 \times 1} \\ \delta_{(J)6 \times 1} \end{Bmatrix}$ as shown in equation (10).

$$\begin{Bmatrix} \delta_{(K)6 \times 1} \\ \delta_{(L)6 \times 1} \end{Bmatrix} = - \begin{bmatrix} K_{22}^{(j1)} + K_{11}^{(e)} & K_{12}^{(e)} \\ K_{21}^{(e)} & K_{22}^{(e)} + K_{11}^{(j2)} \end{bmatrix}_{12 \times 12}^{-1} \begin{bmatrix} K_{12}^{(j1)} & \mathbf{0} \\ \mathbf{0} & K_{21}^{(j2)} \end{bmatrix}_{12 \times 12} \begin{Bmatrix} \delta_{(I)6 \times 1} \\ \delta_{(J)6 \times 1} \end{Bmatrix} \quad (10)$$

Substituting equation (10) into (9) leads to equations of the combined element as shown in equation (11).

$$\left(\begin{bmatrix} K_{11}^{(j1)} & \mathbf{0} \\ \mathbf{0} & K_{22}^{(j2)} \end{bmatrix}_{12 \times 12} - \begin{bmatrix} K_{12}^{(j1)} & \mathbf{0} \\ \mathbf{0} & K_{21}^{(j2)} \end{bmatrix}_{12 \times 12} \begin{bmatrix} K_{22}^{(j1)} + K_{11}^{(e)} & K_{12}^{(e)} \\ K_{21}^{(e)} & K_{22}^{(e)} + K_{11}^{(j2)} \end{bmatrix}_{12 \times 12}^{-1} \begin{bmatrix} K_{12}^{(j1)} & \mathbf{0} \\ \mathbf{0} & K_{21}^{(j2)} \end{bmatrix}_{12 \times 12} \right) \begin{Bmatrix} \delta_{(I)6 \times 1} \\ \delta_{(J)6 \times 1} \end{Bmatrix} = \begin{Bmatrix} F_{(I)6 \times 1} \\ F_{(J)6 \times 1} \end{Bmatrix} \quad (11)$$

The global finite element equations of truss structures can be assembled from the equations of the combined elements from equation (11). After the displacements of external nodes ((I) and (J)) of each element are solved, the displacements of the internal nodes ((K) and (L)) can be solved using equation (10). Then, displacement and stress distribution of each sub-element can be calculated using the traditional frame finite element method demonstrated in [8].

Young's modulus of all joints element are reduced to make the joints more deformable and the behavior of the semi-rigid frame model closer to reality. The Young's modulus of the semi-rigid joints are specified as described in equation (12).

$$E_{joint} = \alpha E_{main\ element} \quad (12)$$

where α is a deformation factor to specify deformability of joint elements. The factor should always be greater than zero but not exceed one.

2.3 Problem definition

Four truss problems, ten-bar, twenty-five-bar, seventy-two-bar, and two-hundred-bar are employed. Further details of truss geometry can be found in [26]. In this article, a joint length is referred to as L_{joint} . All truss members are circular

cross-section members. All joint lengths and cross-section areas in each problem are specified by the same value. The shear modulus is calculated by equation (13).

$$G = E/2(1 + \nu) \tag{13}$$

where, ν is the Poisson’s ratio which is equal to 0.3 in this work.

2.3.1 Ten-bar truss

The ten-bar plane truss is subjected to loading detailed as follows:

$F_y = 50$ kip at nodes 1, 3
 $F_y = -150$ kip at nodes 2, 4

2.3.2 Twenty-five-bar truss

The twenty-five-bar space truss is subjected to loading as follows:

$F_x = 1$ kip, $F_y = 10$ kip, $F_z = -5$ kip at node 1
 $F_y = 10$ kip, $F_z = -5$ kip at node 2
 $F_x = 0.5$ kip at node 3
 $F_x = 0.5$ kip at node 6

2.3.3 Seventy-two-bar truss

The seventy-two-bar space truss is subjected to loading as follows:

$F_x = 5$ kip, $F_y = 5$ kip, $F_z = -5$ kip at node 17

2.3.4 Two-hundred-bar truss

The two-hundred-bar plane truss is subjected to loading as follows:

$F_x = 1$ kip at nodes 1, 6, 15, 20, 29, 34, 43, 48, 57, 62, 71
 $F_y = -10$ kip at nodes 1-6, 8, 10, 12, 14, 16-20, 22, 24, 26, 28-34, 36, 38, 40, 42-48, 50, 52, 54, 56-62, 64, 66, 68, 70-75

where F_x , F_y , and F_z are external loads acting in the x , y , and z -direction, respectively.

3. Results

The finite element results of the proposed semi-rigid frame model are compared to the original truss and frame models. Further details of each test problem are given in Table 1.

Table 1 Details of test problems

Problem	L_{joint} (in)	A (in ²)	α	E (ksi)	ρ (lb/in ³)
10-bar	0.5	20	0.5	1e4	0.1
25-bar	0.5	1	0.5	1e4	0.1
72-bar	0.5	1	0.5	1e4	0.1
200-bar	0.5	10	0.5	3e4	0.283

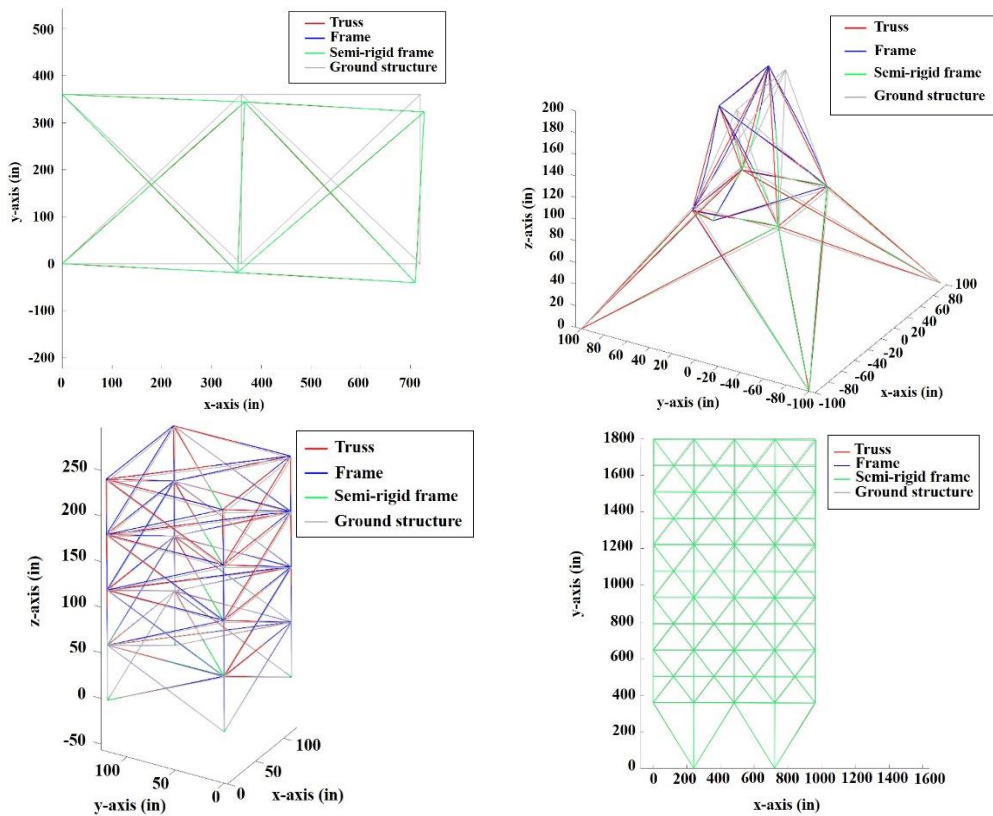


Figure 3 Displacement results of the 10-bar, 25-bar, 72-bar, and 200-bar truss problems

Young’s modulus of joint elements of all tests are reduced to half of modulus of the main elements ($\alpha=0.5$) and the lengths of all joints are specified to be 0.5 in to investigate the behavior of a truss structure with semi-rigid joints. Comparison of the displacement results of the semi-rigid frame, truss and frame finite element models of 10 bar,

25-bar, 72-bar, and 200-bar truss cases are shown in Figure 3. The displacement results of all test cases are enlarged 20 times their actual values. Von Mises stress results of the 10-bar, 25-bar, 72-bar, and 200-bar cases are shown in Figures 4-5, Figures 6-7, Figures 8-9, and Figures 10-11, respectively.

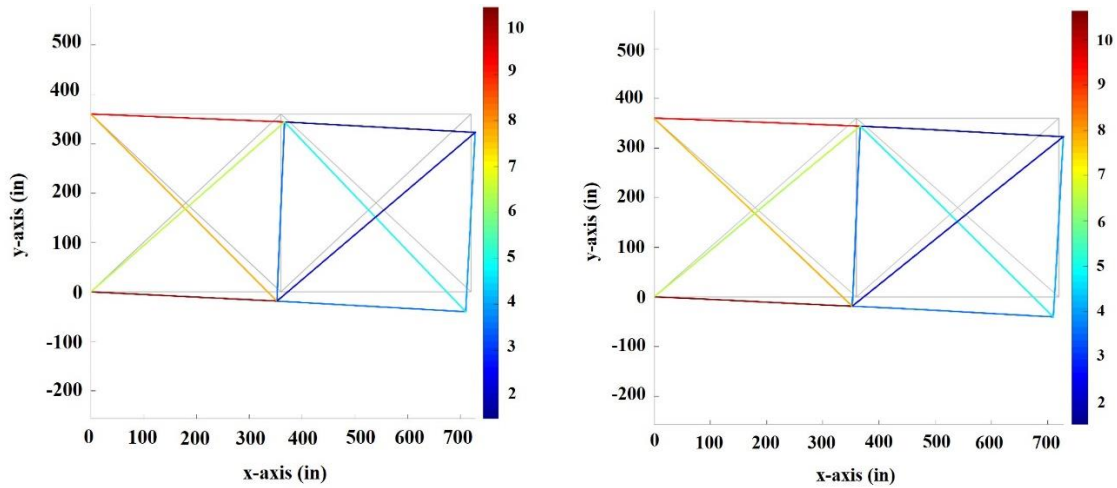


Figure 4 Von Mises stress results of truss (left) and frame (right) finite element models for a 10-bar truss problem

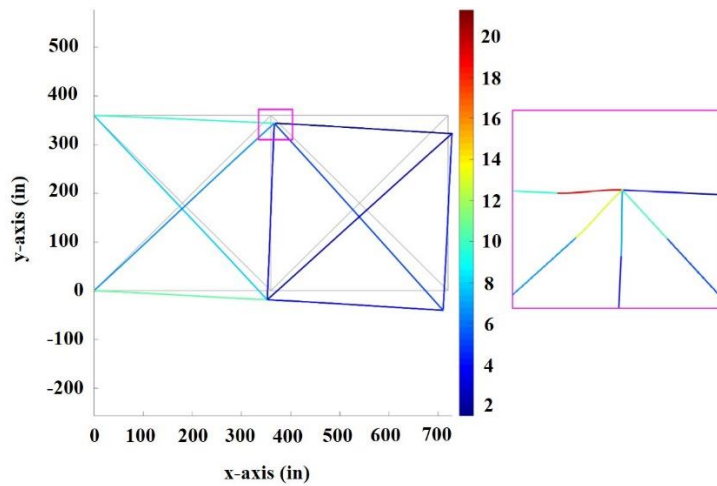


Figure 5 Von Mises stress results of semi-rigid frame finite element models for a 10-bar truss problem

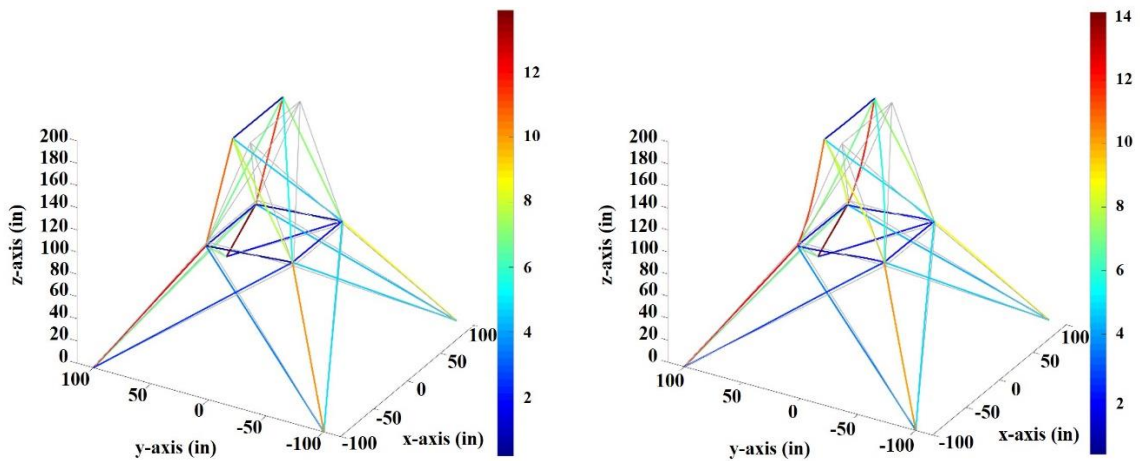


Figure 6 Von Mises stress results of truss (left) and frame (right) finite element models for a 25-bar truss problem

4. Discussion

The displacement distribution of the semi-rigid-joint frame, pinned-joint truss and rigid-joint frame models are very close in all test cases. Each element of the semi-rigid frame and frame models is subjected to a bending moment. Thus, there are also rotational displacements in both models, while only translation displacement occurs in the truss model. However, the maximum Von Mises stress of the

semi-rigid frame model is much greater compared to truss and frame models in all test structures. From the enlarged images in Figures 5, 7, 9, and 11, due to a 50% reduction of Young’s modulus at joint elements, Von Mises stresses at these elements and the main elements are discontinuous. The Von Mises stress at most joint elements in all problems are approximately doubled compared to their corresponding main elements.

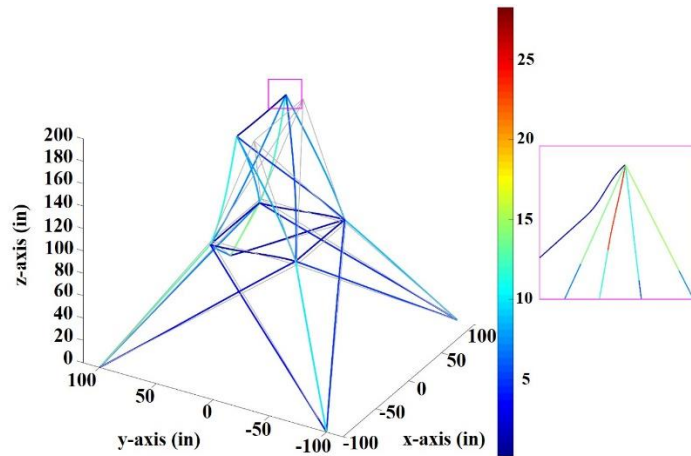


Figure 7 Von Mises stress results of semi-rigid frame finite element models for a 25-bar truss problem

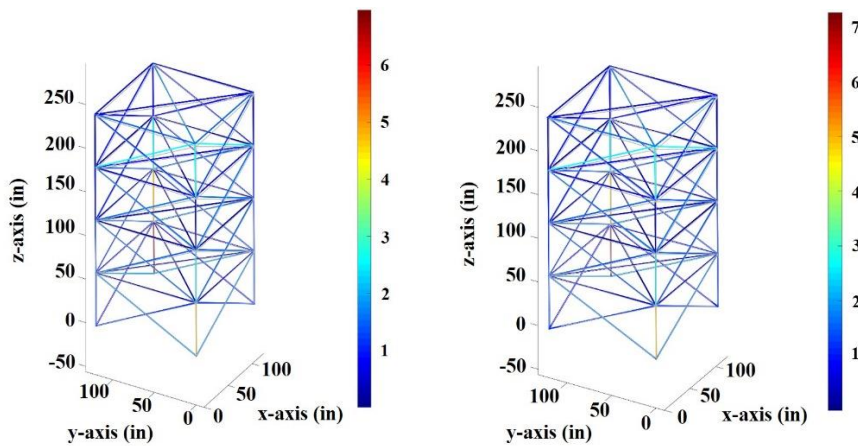


Figure 8 Von Mises stress results of truss (left) and frame (right) finite element models for a 72-bar truss problem

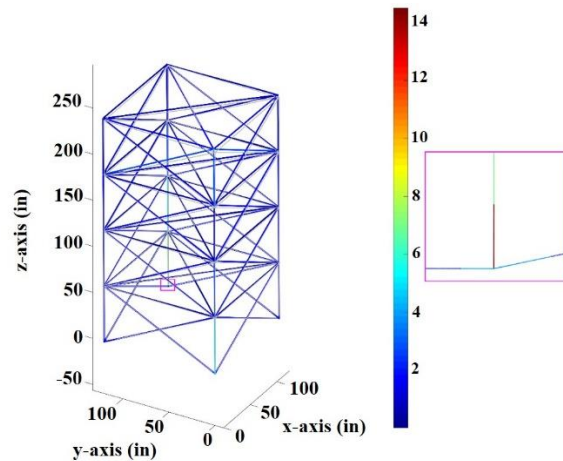


Figure 9 Von Mises stress results of semi-rigid frame finite element models for a 72-bar truss problem

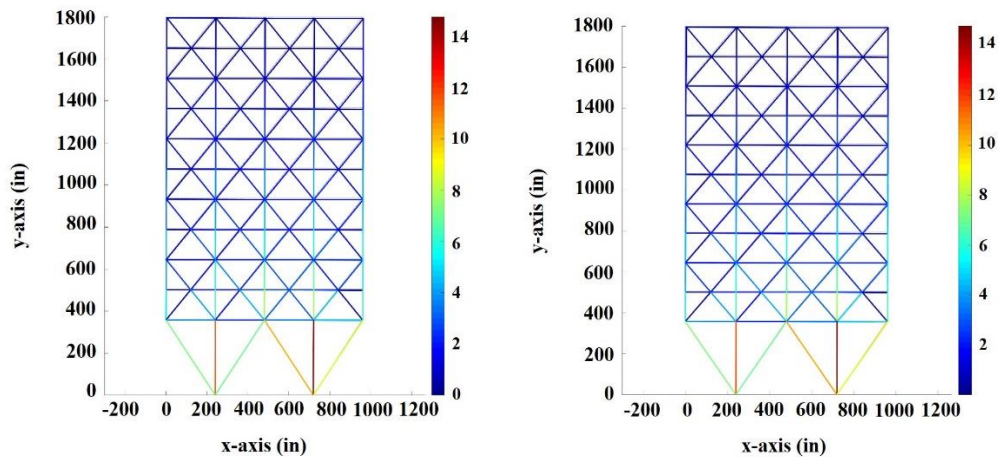


Figure 10 Von Mises stress results of truss (left) and frame (right) finite element models for a 200-bar truss problem

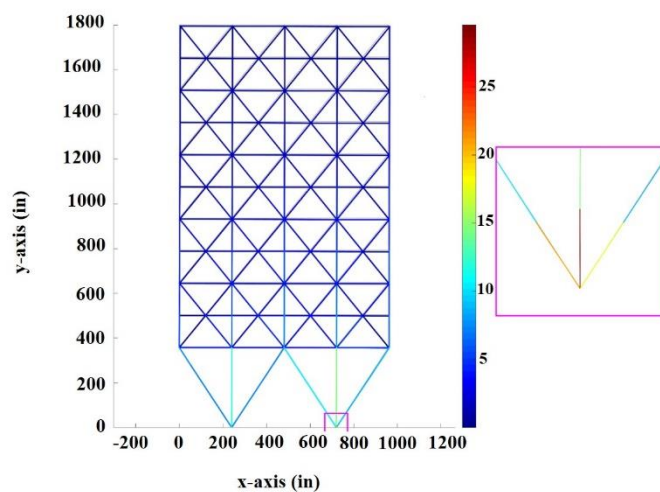


Figure 11 Von Mises stress results of semi-rigid frame finite element models for a 200-bar truss problem

5. Conclusions

An improved finite element method for truss structures with semi-rigid connections was obtained in this research. Overall, the displacement and Von Mises stress distributions of the semi-rigid frame model are close to truss and frame models, except Von Mises stress at joint elements of the semi-rigid frame model. These are much greater compared to their corresponding main elements and from other models. The proposed finite element model simulates the behavior of a semi-rigid joint element that is weaker than its main element. With a 50% reduction of Young's modulus of the joint element, the Von Mises stresses that occur in most joints elements are dramatically increased. This should not be neglected in practical structural design. Compared to truss and frame models, the behavior of the proposed model is more like real truss structures with bolts or welding connections, in which the maximum stress or failure are likely to take place at the joints. The deformation factor (α), which is equal to 0.5, is just a convenient value to investigate a general behavior of the proposed semi-rigid frame model. Experimental work should be done to validate this simulation concept. In updating the finite element model, the α factor for each semi-rigid joint should be an a-priori unknown. Once the experimental results are obtained, the correct values of α for all joints can be found by means of an inverse

problem (e.g., a least squares technique). Moreover, it is more challenging to model these α values as uncertainties or random variables in an optimization problem, which will consequently become a new type of reliability optimization.

6. Acknowledgements

The authors are grateful for support from the Royal Golden Jubilee Ph.D. Program (Grant No. PHD/0130/2557) and the Thailand Research Fund (BRG5880014).

7. References

- [1] Prakotmak P. Finite element based model of parchment coffee drying. *KKU Eng J.* 2015;42(1):39-49.
- [2] Sae-Lee D, Sosakul T, Hovichitr W, Suriyawanakul J, Poovarodom P, Bumrungsiri W, Pongkornkumpon S, Supasatean W. Three dimensional finite element analysis of mandibular premolar restored with fiber post and resin composite with different cavity designs. *KKU Eng J.* 2016;26:43(4):196-203.
- [3] Tejani GG, Savsani VJ, Patel VK. Adaptive symbiotic organisms search (SOS) algorithm for structural design optimization. *J Comput Des Eng.* 2016;3(3):226-49.
- [4] Tejani GG, Savsani VJ, Bureerat S, Patel VK. Topology and size optimization of trusses with static

- and dynamic bounds by modified symbiotic organisms search. *J Comput Civ Eng.* 2017;32(2):1-11.
- [5] Tejani GG, Savsani VJ, Patel VK, Mirjalili S. Truss optimization with natural frequency bounds using improved symbiotic organisms search. *Knowl Base Syst.* 2018;143:162-78.
- [6] Savsani VJ, Tejani GG, Patel VK. Truss topology optimization with static and dynamic constraints using modified subpopulation teaching–learning-based optimization. *Eng Optim.* 2016;48(11):1990-2006.
- [7] Reddy JN. *An introduction to the finite element method.* New York: McGraw-Hill; 1993.
- [8] Rao SS. *The finite element method in engineering.* 6th ed. UK: Butterworth-heinemann; 2017.
- [9] Lui EM, Chen WF. Analysis and behaviour of flexibly-jointed frames. *Eng Struct.* 1986;8(2):107-18.
- [10] Suarez LE, Singh MP, Matheu EE. Seismic response of structural frameworks with flexible connections. *Comput Struct.* 1996;58(1):27-41.
- [11] Hadianfard MA, Razani R. Effects of semi-rigid behavior of connections in the reliability of steel frames. *Struct Saf.* 2003;25(2):123-38.
- [12] Saritas A, Koseoglu A. Distributed inelasticity planar frame element with localized semi-rigid connections for nonlinear analysis of steel structures. *Int J Mech Sci.* 2015;96:216-31.
- [13] Ozel HF, Saritas A, Tasbahji T. Consistent matrices for steel framed structures with semi-rigid connections accounting for shear deformation and rotary inertia effects. *Eng Struct.* 2017;137:194-203.
- [14] Da Silva JG, De Lima LR, Vellasco PD, De Andrade S, De Castro RA. Nonlinear dynamic analysis of steel portal frames with semi-rigid connections. *Eng Struct.* 2008;30(9):2566-79.
- [15] Hadianfard MA, Rahnema H. Advanced nonlinear time-history analysis of partially restrained steel frames by using integrated equations of motion. In: Tizani W, Editor. *Proceedings of the International Conference on Computing in Civil and Building Engineering*; 2010 Jun 30-Jul 2; University of Nottingham, UK. UK: Nottingham University Press; 2010. p. 1-7.
- [16] Galvão AS, Silva AR, Silveira RA, Gonçalves PB. Nonlinear dynamic behavior and instability of slender frames with semi-rigid connections. *Int J Mech Sci.* 2010;52(12):1547-62.
- [17] Minghini F, Tullini N, Laudiero F. Vibration analysis of pultruded FRP frames with semi-rigid connections. *Eng Struct.* 2010;32(10):3344-54.
- [18] Al-Aasam HS, Mandal P. Simplified procedure to calculate by hand the natural periods of semirigid steel frames. *J Struct Eng.* 2012;139(6):1082-7.
- [19] Nguyen PC, Kim SE. Nonlinear elastic dynamic analysis of space steel frames with semi-rigid connections. *J Constr Steel Res.* 2013;84:72-81.
- [20] Reyes-Salazar A, Bojórquez E, Haldar A, López-Barraza A, Rivera-Salas JL. Seismic response of 3D steel buildings considering the effect of PR connections and gravity frames. *Sci World J.* 2014;2014:1-13.
- [21] Lyu N, Saitou K. Decomposition-Based assembly synthesis for structural stiffness. *J Mech Des.* 2003;125(3):452-63.
- [22] Lyu N, Saitou K. Topology optimization of multicomponent beam structure via decomposition-based assembly synthesis. *J Mech Des.* 2005;127(2):170-83.
- [23] Hansen SD, Anderton GL, Connacher NE, Dougherty CS. *Analysis of the 747 aircraft wing-body intersection.* New York: Air Force Institute of Technology; 1968. Report No.: AFFDL TR 68-150.
- [24] Stasa FL. *Applied finite element analysis for engineers.* USA: Oxford University Press; 1985.
- [25] Kohnke P. *Ansys engineering analysis system theoretical manual.* 3rd ed. Houston: Swanson analysis system; 1986.
- [26] Bureerat S, Pholdee N. Optimal truss sizing using an adaptive differential evolution algorithm. *J Comput Civ Eng.* 2015;30(2):04015019.